Finite-temperature Hartree-Fock-Bogoliubov calculations in rare earth nuclei

Alan L. Goodman*
Department of Physics and Quantum Theory Group, Tulane University, New Orleans, Louisiana 70118
(Received 19 May 1986)

The temperature dependence of deformations and pair gaps is calculated for ^{148}Sm, ^{170}Er, and ^{186,188}Os. Increasing the temperature induces a variety of shape phase transitions: prolate and oblate to spherical, triaxial to oblate, and spherical to prolate. Heating also produces the superfluid to normal phase transition.

I. INTRODUCTION

This article considers how the shapes of rare earth nuclei vary with temperature. Recent experiments on giant dipole resonances (GDR's) have increased interest in this subject. The shape of the GDR which is constructed on highly excited states can determine nuclear deformations at high temperatures. One GDR experiment[1] suggests that the prolate ground state deformation of ^{160,166}Er persists for temperatures up to 1 MeV. Another GDR experiment[2] implies that ^{166}Er experiences a shape change and has an oblate deformation at $kT \approx 1.6$ MeV.

The thermal response of deformed rotational nuclei will be contrasted with the response of transitional γ-soft nuclei. Rotational nuclei have static deformations when they are cold because of shell effects. Heating these nuclei washes out the shell effects and eliminates the deformation. However, transitional nuclei may respond quite differently when they are heated. It will be demonstrated that raising the temperature in ^{148}Sm changes a spherical shape into a prolate shape.

Solutions are found for the finite-temperature Hartree-Fock-Bogoliubov (FTHFB) equation. At each temperature the FTHFB equation determines the equilibrium values of the quadrupole deformation parameters β and γ, as well as the pairing gaps Δ_p and Δ_n. Free energy surfaces $F(\beta,\gamma)$ are constructed to see how nuclei change when they depart from their equilibrium states.

The pairing-plus-quadrupole (PPQ) Hamiltonian of Kumar and Baranger (KB) is employed.[3] Consequently our calculations are the finite-temperature extension of the KB static calculations.[4]

There have been previous self-consistent field calculations to determine how the shapes of rare-earth nuclei vary with temperature. Brack and Quentin[5] found that a temperature of 3 MeV was required to eliminate the deformation in ^{168}Yb. Several groups[6-8] have studied ^{164}Er, where the deformation collapses at $kT = 1.4$ MeV.[8]

II. THEORY

The model space is chosen as follows: An inert core is assumed, consisting of 40 protons and 70 neutrons. The active proton shells have $N = 4,5$, which can accommodate 72 protons. The active neutron shells have $N = 5,6$, which can hold 98 neutrons. The proton and neutron oscillator lengths are[3]

$$b_p^2 = b^2/\alpha_p \,, \tag{1}$$

$$b_n^2 = b^2/\alpha_n \,, \tag{2}$$

where

$$b = (\hbar/m\omega)^{1/2} = 1.003A^{1/6} \text{ fm} \,, \tag{3}$$

$$\alpha_p = (2Z/A)^{1/3} \,, \tag{4}$$

$$\alpha_n = (2N/A)^{1/3} \,. \tag{5}$$

The pairing-plus-quadrupole Hamiltonian of Kumar and Baranger[3,4] is

$$H = H_s + H_p + H_Q \,, \tag{6}$$

where

$$H_s = \sum_{j\tau} e_{j\tau} C_{j\tau}^\dagger C_{j\tau} \,, \tag{7}$$

$$H_p = -G_\tau \sum_{\substack{ij>0 \\ \tau}} C_{i\tau}^\dagger C_{\bar{i}\tau}^\dagger C_{\bar{j}\tau} C_{j\tau} \,, \tag{8}$$

$$\begin{aligned} H_Q &= -\tfrac{1}{2}\chi(\alpha_p^2 Q_p + \alpha_n^2 Q_n)(\alpha_p^2 Q_p + \alpha_n^2 Q_n) \\ &= -\tfrac{1}{2}\chi \sum_{\substack{ijkl \\ \tau\tau'}} \sum_M (-1)^M \alpha_\tau^2 \alpha_{\tau'}^2 \langle i\tau | Q_{2M} | k\tau \rangle \\ &\quad \times \langle j\tau' | Q_{2-M} | l\tau' \rangle C_{i\tau}^\dagger C_{j\tau'}^\dagger C_{l\tau'} C_{k\tau} \,, \end{aligned} \tag{9}$$

and i, j, k, and l each denote $nljm$, τ is p or n, $M = 2,1,0,-1,-2$, $\bar{j}$ is the time reverse of j, and

$$Q_{2M} = r^2 Y_{2M}(\theta,\phi) \,. \tag{10}$$

The spherical single-nucleon energies $e_{j\tau}$ are taken from Table 1 in Ref. 4. The strengths of the monopole pair interaction are[4]

$$G_p = \frac{27 \text{ MeV}}{A} \,, \tag{11}$$

$$G_n = \frac{22 \text{ MeV}}{A} \,. \tag{12}$$

The strength of the quadrupole interaction is[4]

$$\chi = \frac{70 \text{ MeV}}{A^{1.4} b^4} \,. \tag{13}$$

Following KB, all matrix elements of Q_{2M} between states

of the upper harmonic oscillator shell ($N=5$ for protons, $N=6$ for neutrons) are multiplied by

$$\zeta=(N+\tfrac{3}{2})/(N+\tfrac{5}{2}) . \tag{14}$$

Since the Hamiltonian (6) does not include the cranking term, $-\omega J_x$, our calculations are restricted to spin zero.

For the PPQ Hamiltonian the finite-temperature HFB equation[9–11] simplifies to coupled finite-temperature Hartree-Fock (FTHF) and finite-temperature Bardeen-Cooper-Schrieffer (FTBCS) equations. The solution is obtained by the following steps:

1. Choose a temperature T.
2. Choose trial values for the quadrupole deformation parameters β and γ.
3. Solve the FTHF eigenvalue equation

$$\mathscr{H}\,|\,\alpha\tau\rangle=\epsilon_{\alpha\tau}\,|\,\alpha\tau\rangle , \tag{15}$$

where the HF Hamiltonian is

$$\mathscr{H}=e+\Gamma , \tag{16}$$

$$\Gamma_{i\tau,j\tau}=-\frac{\hbar\omega\alpha_\tau^2}{b^2}\left[\langle i\tau\,|\,Q_{20}\,|\,j\tau\rangle\beta\cos\gamma+\frac{1}{\sqrt{2}}\langle i\tau\,|\,Q_{22}+Q_{2-2}\,|\,j\tau\rangle\beta\sin\gamma\right] , \tag{17}$$

$$\hbar\omega=\frac{41.2\ \text{MeV}}{A^{1/3}} , \tag{18}$$

the HF orbitals are

$$|\,\alpha\tau\rangle=\sum_i D_{\alpha\tau,i\tau}\,|\,i\tau\rangle , \tag{19}$$

and $\epsilon_{\alpha\tau}$ is the HF single-nucleon energy.

4. Solve the FTBCS equation for the pair gaps Δ_p and Δ_n

$$1=\frac{G_\tau}{2}\sum_{\alpha>0}\frac{\tanh(E_{\alpha\tau}/2kT)}{E_{\alpha\tau}} , \tag{20}$$

where the quasiparticle energy is

$$E_{\alpha\tau}=[(\epsilon_{\alpha\tau}-\mu_\tau)^2+\Delta_\tau^2]^{1/2} , \tag{21}$$

and k is Boltzmann's constant. The chemical potentials μ_p and μ_n are determined by the number constraints

$$N_\tau=2\sum_{\alpha>0}\rho_{\alpha\tau} , \tag{22}$$

where the orbital occupation probability is

$$\rho_{\alpha\tau}=v_{\alpha\tau}^2+(u_{\alpha\tau}^2-v_{\alpha\tau}^2)f_{\alpha\tau} , \tag{23}$$

and

$$v_{\alpha\tau}^2=\tfrac{1}{2}\left[1-\frac{(\epsilon_{\alpha\tau}-\mu_\tau)}{E_{\alpha\tau}}\right]=1-u_{\alpha\tau}^2 , \tag{24}$$

$$f_{\alpha\tau}=\frac{1}{1+e^{E_{\alpha\tau}/kT}} . \tag{25}$$

The Fermi-Dirac factor $f_{\alpha\tau}$ is the probability for thermally exciting a quasiparticle. At zero temperature $f_{\alpha\tau}=0$, and the finite-temperature HFB theory reduces to the zero-temperature HFB theory.

5. Calculate the mass quadrupole moments

$$q_{0\tau}=\sum_\alpha\langle\alpha\tau\,|\,Q_{20}\,|\,\alpha\tau\rangle\rho_{\alpha\tau} , \tag{26}$$

$$q_{2\tau}=\frac{1}{\sqrt{2}}\sum_\alpha\langle\alpha\tau\,|\,Q_{22}+Q_{2-2}\,|\,\alpha\tau\rangle\rho_{\alpha\tau} , \tag{27}$$

$$q_\mu=\sum_\tau q_{\mu\tau}\quad(\mu=0,2) . \tag{28}$$

The factor ζ is included here.

6. For the self-consistent solution, the HF potential and the nucleon density have the same quadrupole deformation. The self-consistency conditions are

$$\hbar\omega\beta\cos\gamma=\chi b^2(\alpha_p^2q_{0p}+\alpha_n^2q_{0n}) , \tag{29}$$

$$\hbar\omega\beta\sin\gamma=\chi b^2(\alpha_p^2q_{2p}+\alpha_n^2q_{2n}) . \tag{30}$$

If these conditions are not satisfied, use the $q_{\mu\tau}$ of Eqs. (26) and (27) together with Eqs. (29) and (30) to define new values of β and γ. Return to step 3, and iterate steps 3–6, until the values of β and γ converge on successive iterations. Then self-consistency is achieved.

7. For each temperature the FTHFB equilibrium solution provides the values of β, γ, Δ_p, Δ_n, μ_p, and μ_n which minimize the free energy

$$F=E-TS , \tag{31}$$

where the energy is

$$E=E_s+E_p+E_Q , \tag{32}$$

$$E_s=\sum_{j\alpha\tau}e_{j\tau}\,|\,D_{\alpha\tau,j\tau}\,|^2\rho_{\alpha\tau} , \tag{33}$$

$$E_p=-\sum_\tau\Delta_\tau^2/G_\tau , \tag{34}$$

$$E_Q=-\tfrac{1}{2}\chi\sum_{\mu=0,2}\left[\sum_\tau\alpha_\tau^2q_{\mu\tau}\right]^2 , \tag{35}$$

and the entropy is

$$S=-2k\sum_{\substack{\alpha>0\\ \tau}}[f_{\alpha\tau}\ln f_{\alpha\tau}+(1-f_{\alpha\tau})\ln(1-f_{\alpha\tau})] . \tag{36}$$

This iterative procedure has been followed to determine the equilibrium state at each temperature. In addition, this algorithm was modified to study nuclear states which deviate from equilibrium. Choose arbitrary values for T, β, and γ. Steps 3, 4, 5, and 7 determine the free energy $F(T,\beta,\gamma)$ of a nonequilibrium state. There are no iterations of these steps. A grid on (β,γ) is chosen, with β varying from 0 to 0.6 in steps of 0.05, and γ varying from 0° to 60° in steps of 10°. The function $F(T,\beta,\gamma)$ is calculated for this grid. The deformation free energy is defined relative to the heated spherical state by

$$F_{\text{def}}(T,\beta,\gamma)=F(T,\beta,\gamma)-F(T,0,0) . \tag{37}$$

III. CALCULATIONS

The FTHFB equations have been solved for a variety of rare earth nuclei.

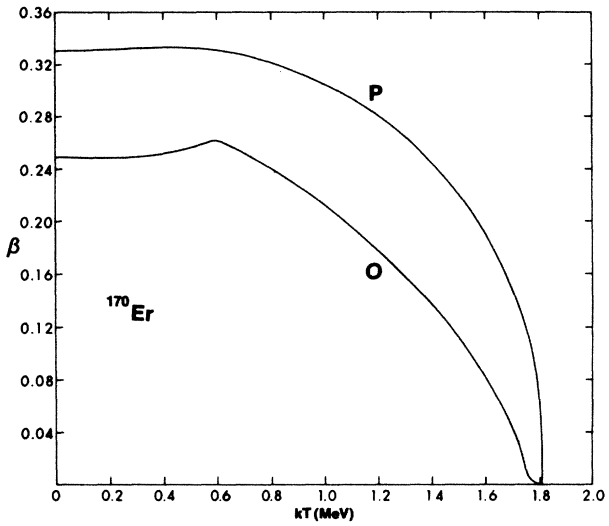

FIG. 1. The quadrupole deformation versus the temperature for the prolate and oblate shapes in ^{170}Er.

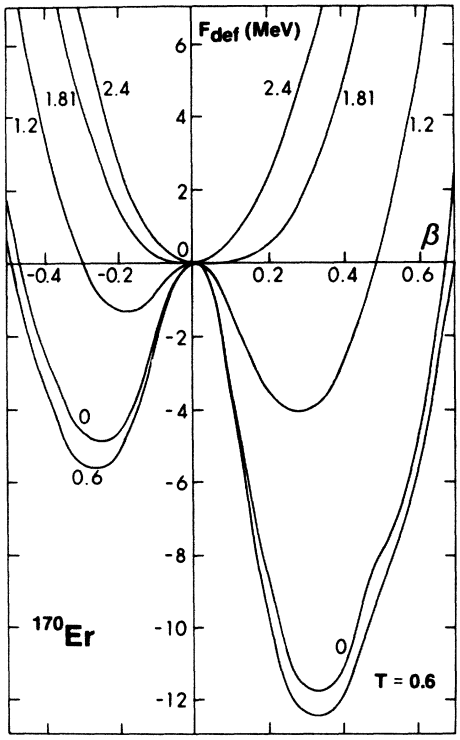

FIG. 2. The deformation free energy versus the quadrupole deformation. Each curve corresponds to a different temperature, which has units of MeV/k. The nucleus is ^{170}Er.

A. ^{170}Er

The nucleus ^{170}Er displays a typical rotational structure. At zero temperature it has an axially symmetric prolate deformation, with a large value of β. It is stable with respect to γ deformations. The equilibrium deformation varies with temperature. The function $\beta(T)$ is shown in Fig. 1 for prolate and oblate shapes. There is a second-order phase transition from a deformed shape to a spherical shape at $kT_c = 1.81$ MeV. The prolate state has a lower free energy than the oblate state for all temperatures below the critical temperature. Therefore the equilibrium shape remains prolate for $T < T_c$.

The deformation free energy $F_{\rm def}(\beta)$ is shown in Fig. 2 for various temperatures. At each temperature the stable equilibrium state is defined by the absolute minimum. These states are prolate, with a positive β. The relative minima with negative β describe the oblate shape. The maxima at $\beta=0$ describe the spherical state. At $T=0$ the prolate state has a deformation $\beta=0.330$, a deformation energy of 11.8 MeV, and a prolate-oblate energy difference of 6.2 MeV. These large magnitudes make ^{170}Er one of the most deformed of the rare earth nuclei. When the temperature is increased to 0.6 MeV, Figs. 1 and 2 show that the equilibrium shape has an increased deformation and deformation free energy. This effect is related to the disappearance of the pair gap Δ. It will be discussed below for ^{148}Sm. For a temperature of 1.2 MeV the potential becomes much shallower and the equilibrium shape is less deformed. At the critical temperature of 1.81 MeV the prolate and oblate minima and the spherical maximum coalesce into a single minimum at $\beta=0$. The equilibrium shape is spherical. The potential is almost flat in the vicinity of $\beta=0$. This is the characteristic behavior of a critical point.

Does the shape remain axially symmetric when the temperature is increased? Consider the contour map of $F_{\rm def}(\beta,\gamma)$ in Fig. 3. This is a plot in polar coordinates, where the radial coordinate is β and the angular coordinate is γ. A prolate shape has $\gamma=0°$ and an oblate shape has $\gamma=60°$. Intermediate values of γ refer to axially asymmetric shapes. The contour lines have constant deformation free energy. The absolute minimum is the dot surrounded by a shaded region. The value of $F_{\rm def}$ at this minimum is given below the temperature. The dot on the $\gamma=60°$ line is the oblate state. Although this state is a minimum in the β direction, it is a maximum in the γ direction. Therefore the oblate state is actually a saddle point. At zero temperature the steep uphill climb from the prolate state to the oblate state indicates a great resistance to γ deformation. When the temperature is raised from 0 to 0.6 and 1.2 MeV, the absolute minimum remains at $\gamma=0°$. Therefore the equilibrium shape remains axially symmetric when the temperature is increased. However, the map for $kT=1.2$ MeV shows that the shape has become softer in both the β and γ directions. For $kT=1.81$ MeV the absolute minimum is at $\beta=0$. The shape is spherical, and evidence of shell structure has almost disappeared.

The effect of heating on the pair gaps is shown in Fig. 4. The neutron pair gap Δ_n vanishes at the critical temperature of 0.39 MeV. The proton pair gap Δ_p disappears at $kT_c=0.47$ MeV. These are second order phase transitions from superfluid phases to normal phases. The ratio $\Delta(T=0)/kT_c$ is 0.57 for protons and 0.63 for neutrons. These are typical values for this phase transition. Observe

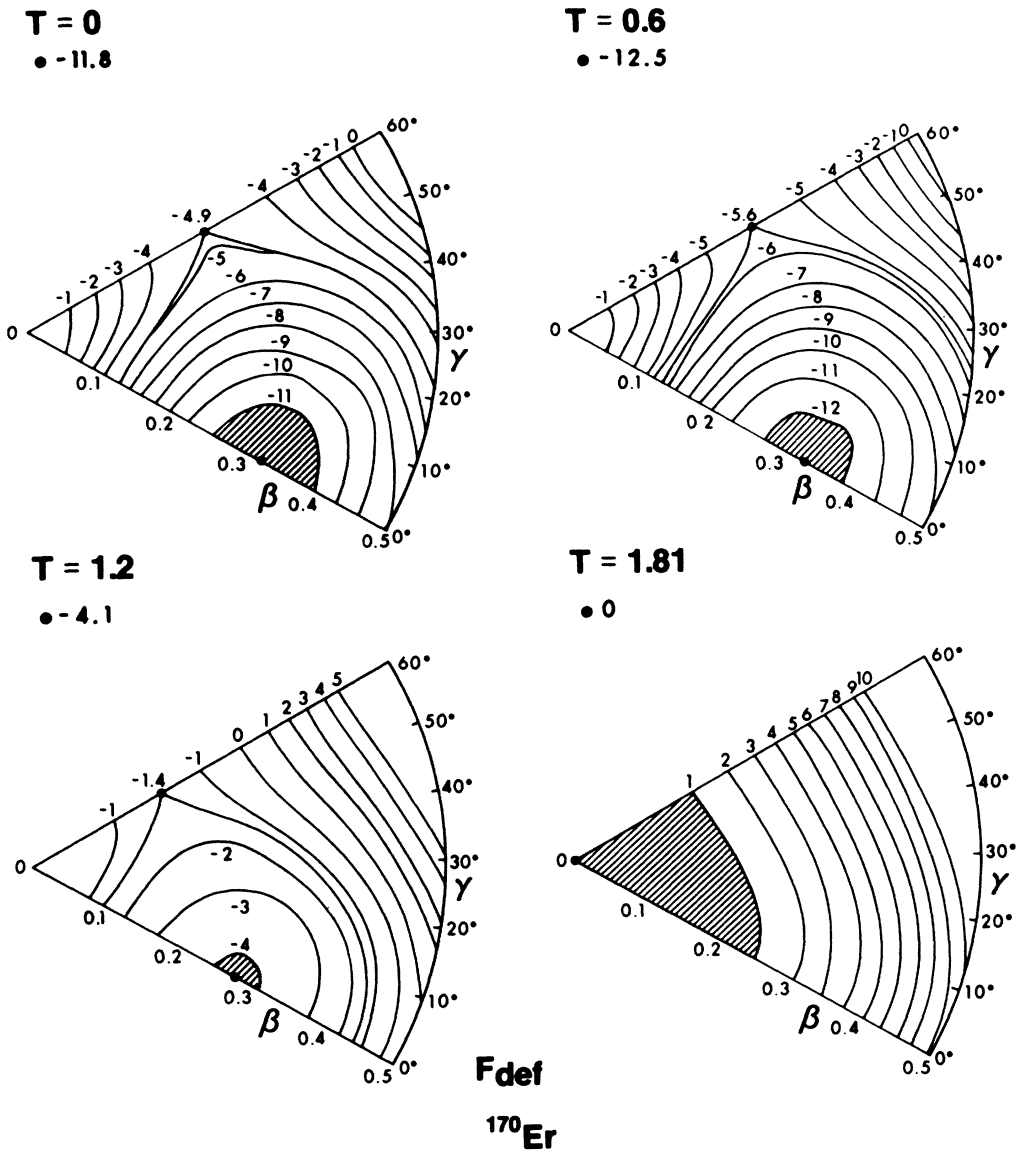

FIG. 3. Contour map of the deformation free energy in the β,γ plane. The lines have constant values of F_{def}. Each map corresponds to a different temperature, which has units of MeV/k. See the text for details. The nucleus is ^{170}Er.

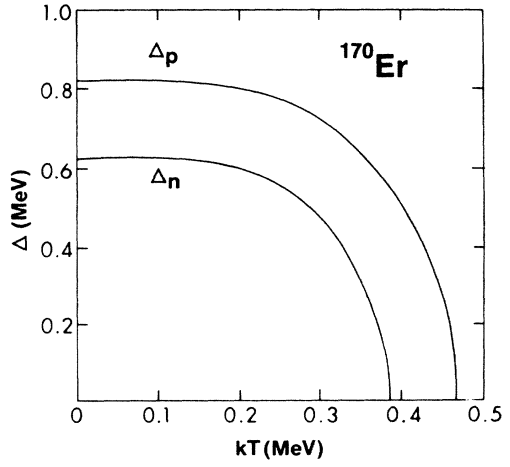

FIG. 4. The proton pair gap and the neutron pair gap versus the temperature for ^{170}Er.

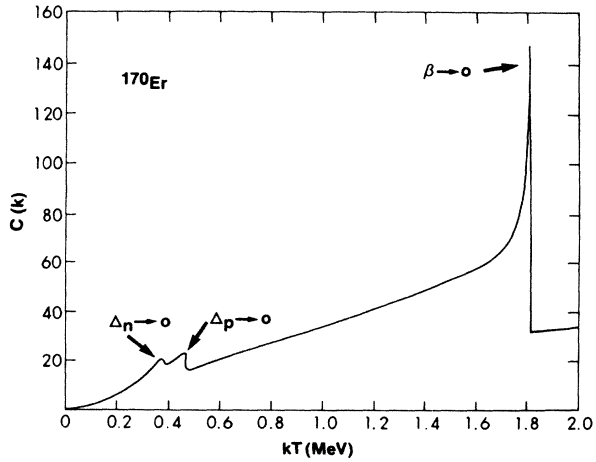

FIG. 5. The specific heat versus the temperature for ^{170}Er.

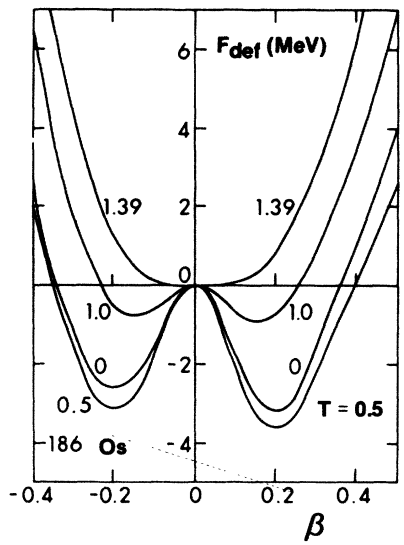

FIG. 6. See Fig. 2. The nucleus is ^{186}Os.

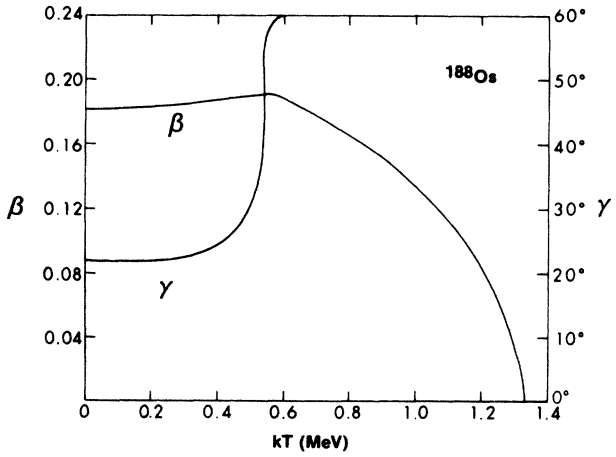

FIG. 8. The quadrupole deformation parameters β and γ versus the temperature for ^{188}Os.

that the critical temperature for destroying the pair gap is much smaller than the critical temperature for eliminating the deformation. This difference will create a dramatic effect in ^{148}Sm.

The specific heat is defined by

$$C=\partial E/\partial T\ . \tag{38}$$

The function $C(T)$ is shown in Fig. 5. The characteristic signature of a second order phase transition is a spike in $C(T)$. There is a large spike when the deformation vanishes, and two smaller spikes when the neutron and proton pair gaps are eliminated.

B. ^{186}Os

We next consider the transitional nucleus ^{186}Os. At zero temperature the static shape is axially symmetric and prolate. However, the prolate state is only 0.5 MeV below the oblate state. Therefore this nucleus is very soft in the γ direction. By raising the temperature the possibility exists that the oblate shape might fall below the prolate, producing a phase transition from a prolate to an oblate shape. However, Fig. 6 shows that this does not happen. At each temperature the prolate deformation has a free energy which is slightly below that of the oblate deformation. So ^{186}Os remains prolate for temperatures up to 1.39 MeV, where the shape becomes spherical. Although the oblate state is a minimum in the β direction, it is a maximum in the γ direction. Therefore the oblate state is a saddle point. The equilibrium deformation $\beta(T)$ for the prolate and oblate shapes is given in Fig. 7.

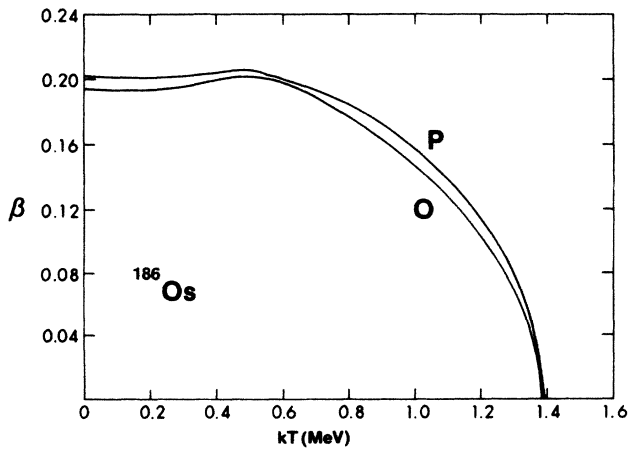

FIG. 7. The quadrupole deformation versus the temperature for the prolate and oblate shapes in ^{186}Os.

C. ^{188}Os

The transitional nucleus ^{188}Os has an axially asymmetric shape at zero temperature. It is extremely soft in the γ direction. The effect of heating on the equilibrium shape is shown in Fig. 8. The value of γ at $T=0$ is 22°, which is a large deviation from axial symmetry. When the temperature is increased to 0.55 MeV, γ suddenly rises, and $\gamma=60°$ at $kT=0.60$ MeV. There is a phase transition from a triaxial shape to an oblate shape. An additional increase in temperature to 1.33 MeV causes β to vanish. This is a transition from an oblate shape to a spherical shape.

Figure 9 depicts the deformation free energy in the β,γ plane. Even at zero temperature this nucleus is γ unstable. The equilibrium state is triaxial with $\beta=0.181$ and $\gamma=22°$. The prolate state at $\beta=0.181$ and $\gamma=0°$ is only 0.04 MeV above the triaxial state. The oblate state at $\beta=0.181$ and $\gamma=60°$ is 0.13 MeV above the triaxial state. When the temperature is 0.55 MeV, the free energy is essentially independent of γ. For $kT=1.33$ MeV the minimum is at $\beta=0$. The shell structure is washed out, and the contours resemble those of a spherical liquid drop.

D. ^{148}Sm

The preceding examples show how raising the temperature changes a deformed shape to a spherical shape. The

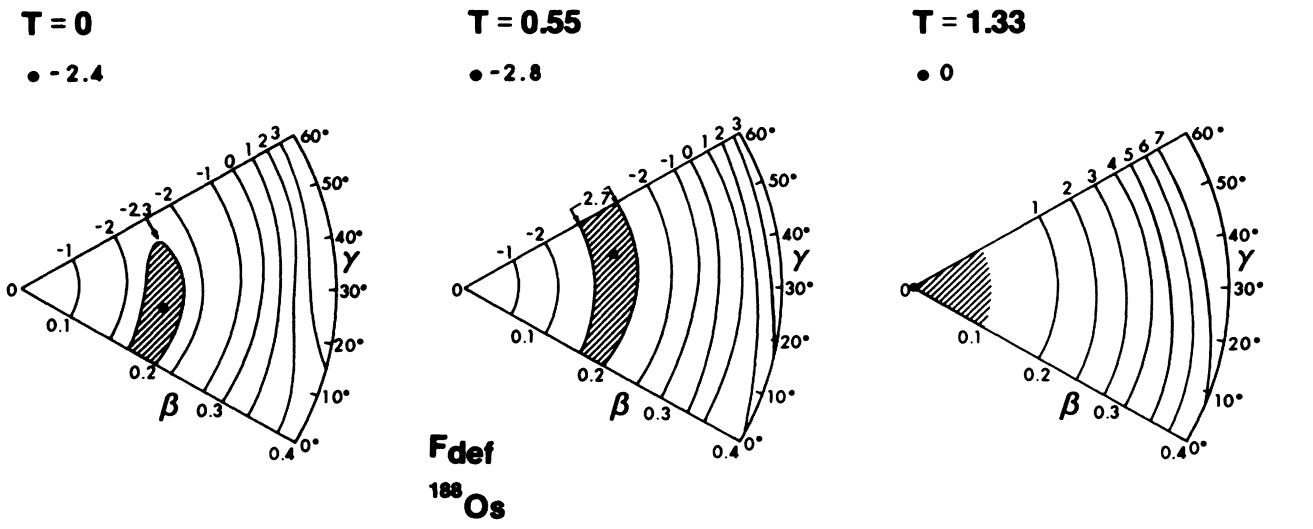

FIG. 9. See Fig. 3. The nucleus is ^{188}Os.

transitional nucleus ^{148}Sm illustrates the inverse effect. Although this nucleus is spherical at zero temperature, heating induces a quadrupole deformation. Since a detailed description of this effect has been published in the form of a Rapid Communication,[12] only a summary will be given here.

Figure 10 shows how β varies with temperature. The shape is spherical for $kT < 0.40$ MeV. When the temperature is increased above 0.40 MeV, the shape suddenly changes from spherical to prolate. When $kT = 0.91$ MeV the shape reverts from prolate back to spherical.

Does this transitional nucleus remain axially symmetric when it acquires a deformation? The free energy contours in the β,γ plane are given in Fig. 11. For temperatures of 0 and 0.4 MeV, the equilibrium minimum occurs at $\beta = 0$. For $kT = 0.6$ MeV, the minimum shifts to $\beta = 0.14$ and $\gamma = 0°$. The equilibrium shape is axially symmetric. There is a free energy barrier of 1.2 MeV separating the prolate minimum from the oblate state. Consequently the shape is not γ unstable, but it is relatively soft in the γ direction.

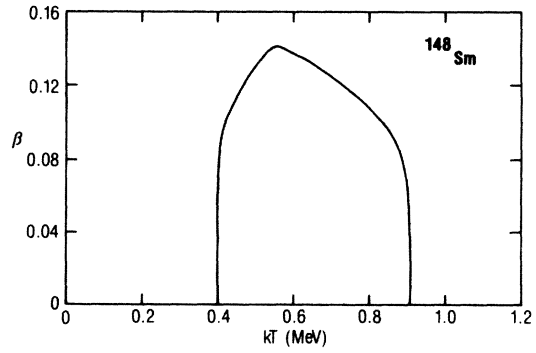

FIG. 10. The quadrupole deformation versus the temperature in ^{148}Sm.

There is also a phase transition from superfluid to normal when Δ vanishes at the critical temperature T_c. For protons T_c is 0.90 MeV/k and for neutrons it is 0.56 MeV/k.

Why does ^{148}Sm display the inverse shape transition from spherical to prolate at $kT = 0.40$ MeV? The ground state of ^{148}Sm is spherical because the monopole pair interaction (which favors spherical shapes) is slightly more effective than the quadrupole interaction (which favors deformed shapes). The critical temperature for eliminating deformation is higher than the critical temperature for removing neutron pairing. For temperatures between these two critical values, the quadrupole interaction can create a deformation. In summary, the relative effectiveness of the symmetry restoring and the symmetry breaking components of the interaction is inverted, simply by raising the temperature.

Would an interaction which is more sophisticated than the pairing-plus-quadrupole also create temperature-induced deformations? For example, suppose that the interaction included quadrupole pairing. It has been shown that [13] for ^{24}Mg the pair gap survives to higher temperatures if quadrupole pairing is included. If the critical temperature for pairing collapse approaches that of deformation collapse, then the temperature-induced deformation effect would disappear. However, if this should occur in ^{148}Sm, then the effect might reappear in ^{150}Sm. This is because (a) the presence of quadrupole pairing actually increases the monopole pair gap,[13] which might give ^{150}Sm a spherical ground state, and (b) the two extra neutrons should increase the critical temperature for deformation collapse. Detailed calculations are required to test these conjectures.

Less dramatic examples of temperature-induced deformation are shown in Fig. 1 for ^{170}Er, Fig. 7 for ^{186}Os, and Fig. 8 for ^{188}Os. For these deformed nuclei, there are small increases in β at the temperature where the pair gap is vanishing. Smith *et al.*[14] have shown that heating the transitional nucleus ^{116}Sn induces a spherical to deformed

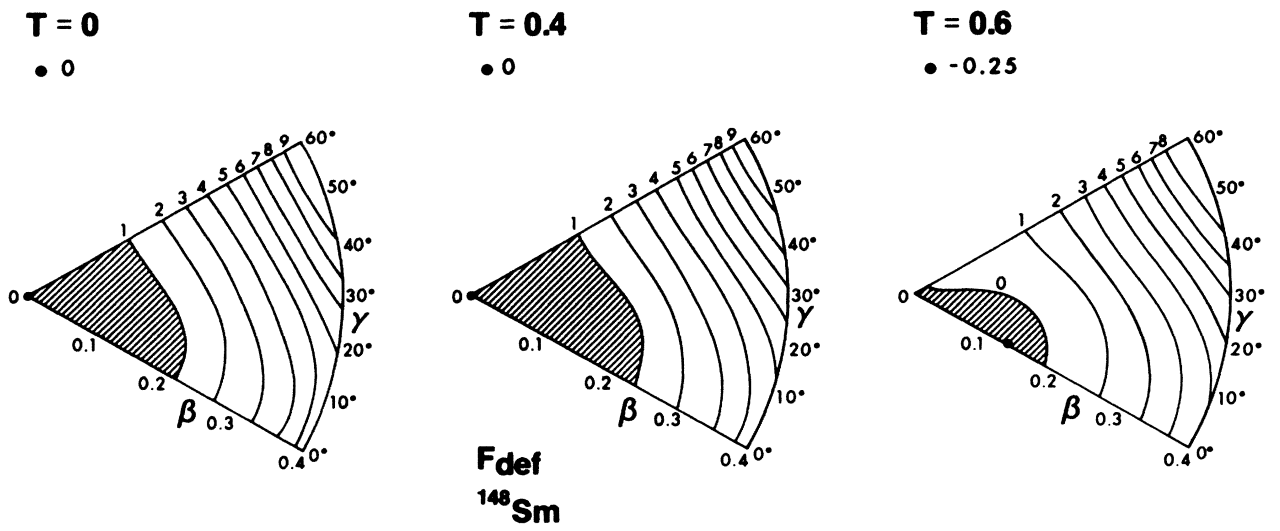

FIG. 11. See Fig. 3. The nucleus is ^{148}Sm.

shape transition.

How can these shape transitions be detected? One possibility is to look at level densities. The FTHFB level density is[11]

$$\rho=\frac{e^{S/k}}{\left[2\pi\sum_{\alpha\tau}E_{\alpha\tau}^2 f_{\alpha\tau}(1-f_{\alpha\tau})\right]^{1/2}}\ . \tag{39}$$

Figure 12 shows the entropy $S(T)$ and the logarithm of the level density $\rho(T)$. The upturn in the level density at very low temperatures is a common failing of level densities which are derived with the saddle-point approximation. Both curves have discontinuities in their slopes at the spherical to prolate transition and at the prolate to spherical transition. This is characteristic of second order phase transitions. Since an alternative definition of the specific heat is

$$C=T(\partial S/\partial T)\ , \tag{40}$$

it follows that $C(T)$ has spikes at the two shape transitions. However, if the energy rather than the temperature is chosen as the independent variable, then the functions $S(E)$ and $\ln\rho(E)$ do not have discontinuities in their slopes at the two shape transitions.

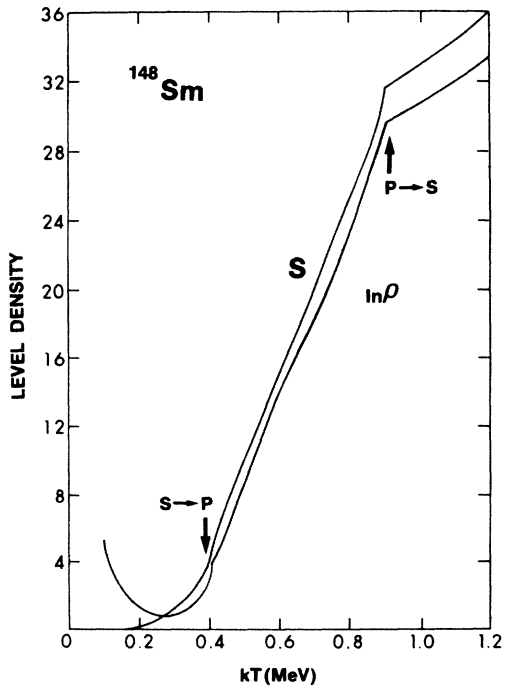

FIG. 12. The entropy S and the logarithm of the level density ρ vs the temperature for ^{148}Sm.

IV. CONCLUSIONS

The finite-temperature HFB equations have been solved for several rare-earth nuclei. The temperature dependence of the shapes and pair gaps is determined. All nuclei display a transition from superfluid to normal when the pair gap Δ vanishes. The critical temperature T_{cp} for the proton transition is approximately $0.5-0.6\,\Delta_p$ $(T=0)$. Similarly the neutron transition occurs at T_{cn} $\simeq 0.5-0.6\,\Delta_n$ $(T=0)$.

There are a variety of shape transitions. The nucleus ^{170}Er has a large prolate deformation at zero temperature. The shape changes from prolate to spherical at $kT=1.81$ MeV. The transitional nuclei ^{186,188}Os are γ unstable. In ^{188}Os the ground state shape is triaxial. There is a transition to an oblate shape at $kT=0.60$ MeV, and another transition to spherical at $kT=1.33$ MeV.

The most exotic shape transition occurs in ^{148}Sm. Although the shape is spherical for temperatures below 0.40 MeV, there is a transition to a prolate shape at $kT=0.40$ MeV, followed by another transition back to spherical at $kT=0.91$ MeV. The first shape transition is created by two conditions. First, the quadrupole-quadrupole interaction and the pairing interaction are delicately balanced in this nucleus, with the latter slightly favored in the ground

state. Second, the critical temperature for the neutron pairing collapse is less than the critical temperature for the deformation collapse.

Our calculations do not include angular momentum projection. Zero-temperature calculations[15] show that when the unprojected energy surface is almost γ unstable, angular momentum projection yields energy surfaces with well-defined triaxial minima. Furthermore, if the angular momentum fluctuation energy is removed from the deformed shape, then the energy balance of the spherical and deformed shapes could be altered, thereby affecting the temperature-induced deformation phenomenon.[16]

ACKNOWLEDGMENTS

The author is grateful to J. L. Egido for useful discussions. This work was supported in part by the National Science Foundation.

[1]C. A. Gossett, K. A. Snover, J. A. Behr, G. Feldman, and J. L. Osborne, Phys. Rev. Lett. **54**, 1486 (1985).
[2]J. J. Gaardhoje, C. Ellegaard, and B. Herskind, Phys. Rev. Lett. **53**, 148 (1984).
[3]M. Baranger and K. Kumar, Nucl. Phys. **A110**, 490 (1968).
[4]K. Kumar and M. Baranger, Nucl. Phys. **A110**, 529 (1968).
[5]M. Brack and P. Quentin, Phys. Scr. **A10**, 163 (1974).
[6]K. Sugawara-Tanabe, K. Tanabe, and H. J. Mang, Nucl. Phys. **A357**, 45 (1981).
[7]J. L. Egido, P. Ring, and H. J. Mang, Nucl. Phys. **A451**, 77 (1986).
[8]C. O. Dorso, J. L. Egido, J. O. Rasmussen, and P. Ring (unpublished).
[9]A. L. Goodman, Nucl. Phys. **A352**, 30 (1981).
[10]M. Sano and M. Wakai, Prog. Theor. Phys. **48**, 160 (1972).
[11]K. Tanabe, K. Sugawara-Tanabe, and H. J. Mang, Nucl. Phys. **A357**, 20 (1981).
[12]A. L. Goodman, Phys. Rev. C **33**, 2212 (1986).
[13]K. Muhlhans, E. M. Muller, U. Mosel, and A. L. Goodman, Z. Phys. A **313**, 133 (1983).
[14]B. C. Smith, F. N. Choudhury, and S. Das Gupta, Phys. Rev. C **17**, 318 (1978).
[15]A. Hayashi, K. Hara, and P. Ring, Phys. Rev. Lett. **53**, 337 (1984).
[16]R. Hilton, private communication.